Applied Surface Science 364 (2016) 931–937

Contents lists available at ScienceDirect

Applied Surface Science

journal homepage: www.elsevier.com/locate/apsusc

High performance hybrid rGO/Ag quasi-periodic mesh transparent electrodes for flexible electrochromic devices

A.S. Voronin[a,b,*], F.S. Ivanchenko[a], M.M. Simunin[d], A.V. Shiverskiy[a], A.S. Aleksandrovsky[c], I.V. Nemtsev[b], Y.V. Fadeev[a], D.V. Karpova[a], S.V. Khartov[b]

[a] Siberian Federal University, 660041 Krasnoyarsk, Russia
[b] Krasnoyarsk Scientific Center, Siberian Branch, Russian Academy of Sciences (KSC SB RAS), 660036 Krasnoyarsk, Russia
[c] L.V. Kirensky Institute of Physics, Siberian Branch, Russian Academy of Sciences, 660036 Krasnoyarsk, Russia
[d] National Research University "MIET", 124498 Moscow, Zelenograd, Russia

ARTICLE INFO

Article history:
Received 9 August 2015
Received in revised form 2 December 2015
Accepted 22 December 2015
Available online 25 December 2015

Keywords:
Quasi-periodic mesh transparent electrode
self-organized template
Reduced graphene oxide (rGO)
Flexible electrochromic device

ABSTRACT

A possibility of creating a stable hybrid coating based on the hybrid of a reduced graphene oxide (rGO)/Ag quasi-periodic mesh (q-mesh) coating has been demonstrated. The main advantages of the suggested method are the low cost of the processes and the technology scalability. The Ag q-mesh coating is formed by means of the magnetron sputtering of silver on the original template obtained as a result of quasi-periodic cracking of a silica film. The protective rGO film is formed by low temperature reduction of a graphene oxide (GO) film, applied by the spray-deposition in the solution of $NaBH_4$. The coatings have low sheet resistance (12.3 Ω/sq) and high optical transparency (82.2%). The hybrid coatings are characterized by high chemical stability, as well as they show high stability to deformation impacts. High performance of the hybrid coatings as electrodes in the sandwich-system «electrode–electrochromic composition–electrode» has been demonstrated. The hybrid electrodes allow the electrochromic sandwich to function without any visible degradation for a long time, while an unprotected mesh electrode does not allow performing even a single switching cycle.

1. Introduction

Transparent conductive coatings based on metal nanowire film and metal mesh coatings obtained by various lithography methods [1–7], can be considered as one of the most promising classes of transparent electrodes due to a combination of low sheet resistance (<15 Ω/sq), high optical transparency (>85%) and flexibility. They are considered to be perspective electrode systems for high performance photovoltaics [8], flexible displays (including sensor displays) [5,9], and electrochromic systems («smart glass») [10]. However, electrodes based on the most available and technological metals (Cu, Ag, Al) have low chemical stability and they are not applicable in aggressive exploitation conditions, for example, in the functioning conditions of electrochromic devices [11]. For the stabilization of mesh transparent electrodes different variants of protection are used, e.g., oxide materials IZO [12], AZO [13]. The shortcoming is in the fact that oxide passivation is associated with vacuum processes, which considerably increases the cost of the coating.

As to galvanic metallization with nickel [14] and platinum [15], the main problem of the considered protection type is the porosity of the thin galvanic coatings resulting in the loss of the system functionality. The system can be stabilized only with the thickness of the galvanically deposited metal being sufficiently large, which is not acceptable due to unsatisfactory optical parameters of the coatings.

Graphene is one of the most perspective materials for creating stable hybrid transparent coatings on the basis of metal mesh structures; in [16,17] a possibility of stabilization using a continuous graphene monolayer is demonstrated. However, such a method of protection is rather costly, though it allows protecting the metal mesh, with the loss of transparency being only about 2.3% [18]. The protective film based on rGO seems far more simple and technological, though there are objective difficulties in forming this protective coating; in particular, the application of a uniform continuous GO layer; in [11,19] the protective film was applied by spin coating, which negatively influences scalability.

The present study suggests a method of forming hybrid transparent conductive coatings based on the hybrid system rGO/Ag q-mesh. The advantages of the method are its two low cost (the

* Corresponding author at: Siberian Federal University, Instrumentation and nanoelectronics, Svobodny pass. 79, 660041 Krasnoyarsk, Russian Federation. Tel.: +7 9029741592.
E-mail address: a.voronin1988@mail.ru (A.S. Voronin).

http://dx.doi.org/10.1016/j.apsusc.2015.12.182
0169-4332/

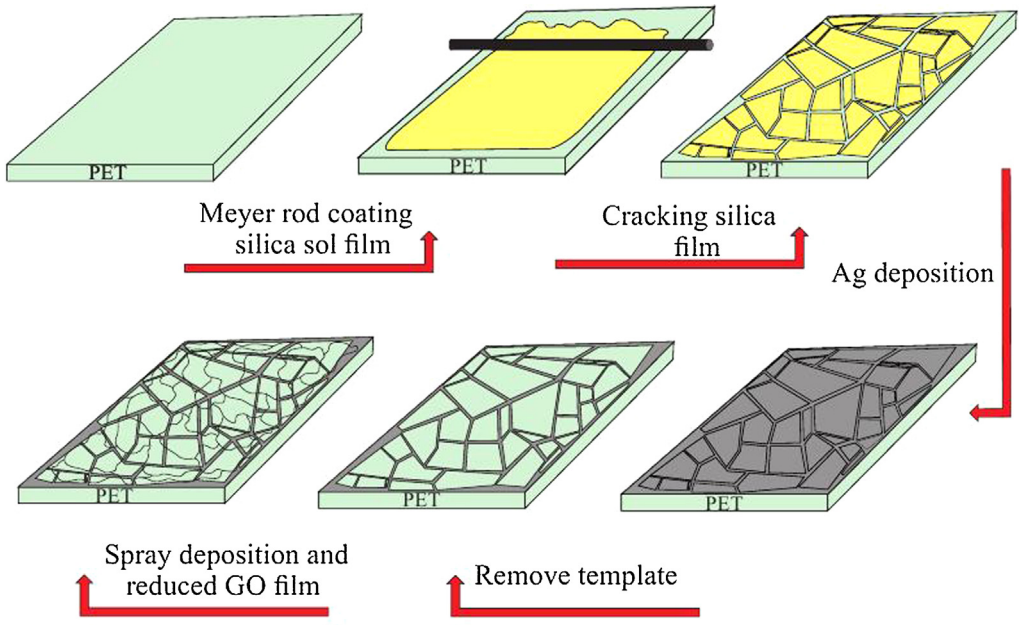

Fig. 1. The formation scheme of the hybrid rGO/Ag q-mesh coating.

estimated cost of the Ag q-mesh coating, 10 $/m^2) and the possibility of the coating formation in the roll-to-roll process. In the first process the transparent Ag q-mesh coating is formed using a crack template [6,7]. An original template suggested by our group is characterized by the absence of blind cracks, missing clusters and high purity of the crack bottom, which allows one to obtain mesh coatings with high characteristics (8.1 Ω/sq at 87.4% transparency, whereas in [7] the value 11 Ω/sq at 86% transparency was obtained, and in [6] the parameter value was 4.2 Ω/sq at 82% transparency). It is also worth noting that the Ag q-mesh coating is characterized by high optical quality and uniformity. In the second process, using the spray-method and low temperature chemical reduction in the $NaBH_4$ solution a thin protective rGO film is formed.

2. Experimental

2.1. Preparation of the quasi-periodic Ag mesh

The process of forming a hybrid transparent coating consists of five stages (Fig. 1): the first stage is the application of a silica sol onto a substrate. To obtain the silica sol, 3 ml of $(C_2H_5O)_4Si$ (TEOS) and 1.5 ml of ethanol were mixed in a test tube while 1.5 ml of water and 0.1 ml of HCl was mixed in another test tube, with these two mixtures being further combined and intensively stirred for 10 min. The pH of the resulting sol was equal to 2. The sol was applied on polymer substrates (PET, 125 μm thick) with the area of 25 cm^2 using a Meyer rod [20]. The calculation thickness of the liquid film being formed amounted to 36.6 μm.

At the second stage, the silica film is dried in air for 15 min at relative humidity of 35–40% and temperature of 20 °C, resulting in the complete cracking of the film. The cracking of the silica film is due to the increase of the system viscosity (owing to the evaporation of the solvent) a pair of two opposed forces appears—one of them tends to mechanically compress the layer in the substrate plane, the second one hinders it (adhesion to the substrate) [21]. With the humidity decreasing (<20%), the dispersion medium is more intensively removed, increasing the probability of their arising defects of the «missing» cluster type.

Besides, the bottom of the gaps is clean without any considerable traces of the working substance. The result of the silica film cracking is presented in Fig. 2. The obtained template is characterized by a high degree of uniformity and a low number of defects. The template has the mean cluster size of 78.7 ± 25.2 μm (Fig. 2c) and the mean crack width of 1.4 ± 0.5 μm (Fig. 2d). The method allows varying the template parameters by varying the sol pH and the liquid film thickness.

At the third stage the magnetron sputtering of a thin silver film is carried out. The silver film was sputtering using the facility «Caroline D15» («ESTO – vacuum», Russia). The film thickness ranged from 70 to 210 nm.

At the fourth stage the template was selectively removed by washing in a 0.1 M solution of KOH at room temperature for 1–2 min in order to completely remove the clusters containing amorphous silica. The described technique allows one to selectively etch away the silica template from the Ag q-mesh. As a result, only the Ag q-mesh remains on the PET substrate. (Fig.A1).

2.2. Preparation of the rGO protective coating

The formation of the rGO protective film was the last stage of forming the hybrid transparent electrode. To form a protective film on Ag q-mesh coating a 1.5% GO solution («Akko Lab», Russia) prepared by the Hummers method [22] was used. A colloidal GO solution was applied by the spray-method on to PET substrates with the Ag q-mesh coating. The thickness of the GO film was set by the amount of the solution per a unit of area. To improve the wettability of the PET substrates by the GO solution the polymer surface was treated with cold plasma, this procedure allows obtaining more integrate films. After spray deposition the graphene oxide films were dried in air at T = 80 °C for 2 h to remove the moisture and form a continuous protective film in the process of GO reduction. The reduction of GO film was carried out in a 0.15 M aqueous solution of $NaBH_4$ for 50 min [23]. After the reduction the system was washed with distilled water and dried in air at T = 70 °C for 1 h.

2.3. Fabrication of an electrochromic device

The hybrid coatings were tested as electrodes in a thin electrochromic device, with the electrodes having the following

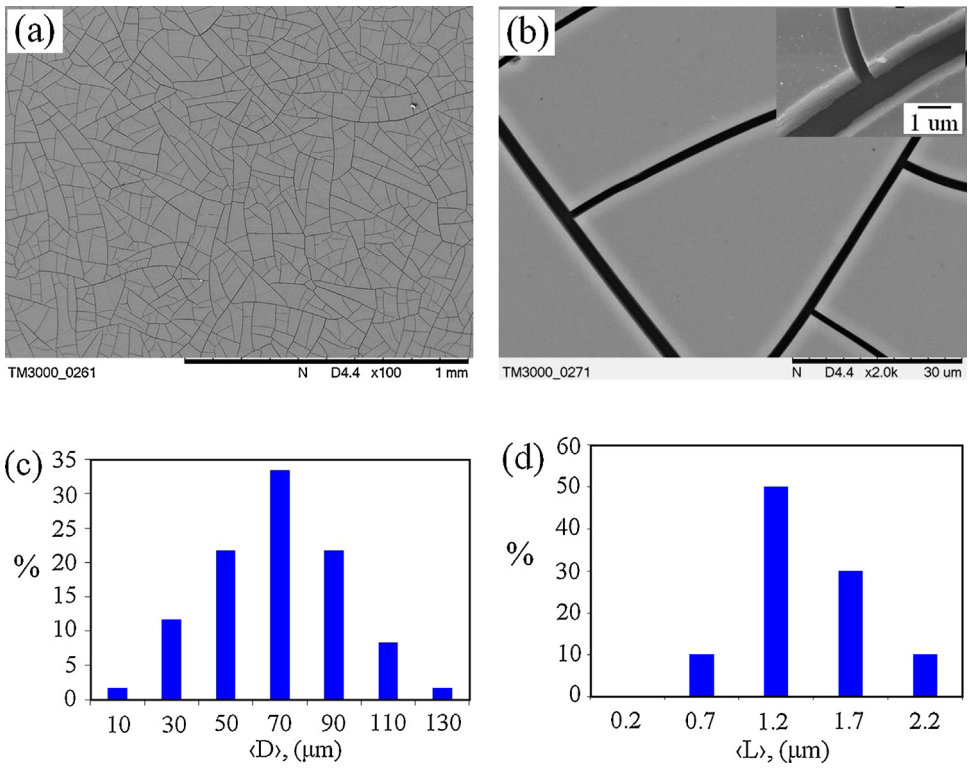

Fig. 2. The result of quasiperiodic cracking of the silica film: clusters (a) and cracks (b) images. The results of statistical processing of the clusters and cracks (c and d).

parameters: 11.4 Ω/sq at 81.4% transparency and 11.7 Ω/sq at 82.1% transparency, respectively. The electrochromic device was fabricated on the basis of a commercial polymer electrochromic composition («iGlass» Ltd, Novosibirsk). The electrochromic composition has high viscosity, preventing the etching component from penetrating under the rGO protective layer. A droplet of the polymer composition was placed on one of the electrodes, covered with the other one and placed under press for an hour (the pressure being 1 kg/cm^2). The layer thickness of the elecrochromic composition was set by spacers and amounted to about 100 μm. The total thickness of the electrochromic device was 350 μm and its transparency—60% at the wavelength of 550 nm.

2.4. Characterization

The morphology of the silica templates and coating was studied by the method of electron microscopy using Hitachi TM 3000 and Hitachi S 5500 (all images obtined in Centers for collective use, KSC SB RAS). The spectral dependencies of the optical transmittance of the Ag q-mesh and hybrid coatings, GO and rGO films and electrochromic device were measured in the range of 400–800 nm with a spectrophotometer Shimadzu UV-360. The Raman spectra of GO and rGO films were measured using a spectrometer Horiba Jobin Yvon T64000 in the range of 20–2800 cm^{-1}. The influence of the mechanical deformations and chemical treatment on the electrical characteristics of the coatings was studied using a laboratory stand.

3. Results and discussion

In the reduction process the GO film significantly loses its transparency and changes its color from yellow-brown to dark grey. Fig. 3a shows the spectral dependences of optical transmittance of GO and rGO films with the concentration of 0.01 ml/cm^2. An acceptable option for passivating a mesh electrode is a thin protective rGO film with the mean transparency being 92–93%. Using thicker rGO films results in a more considerable loss of transparency (Fig.A2). When decreasing the thickness of rGO film, there appear unprotected parts of the mesh, which leads to a significant degradation of the electrodes.

Fig. 3b presents the Raman spectra of GO and rGO. According to the evidence of Raman spectroscopy there are two main peaks in the GO and rGO spectra: G-line, characterizing the vibrations of the system of sp^2 carbon bonds (~1580 cm^{-1}) (graphite-like zone), and 2D-line (~2700 cm^{-1}), which is the overtone of the D-line (defect zone) (~1330 cm^{-1}). The appearance of the D-line for the GO and rGO samples evidences the formation of a defect structure as related to graphite while the regular peak appearing in the range of 2700 cm^{-1} provides evidence for a small number of layers in the rGO structure [24].

The SEM images of the Ag q-mesh and hybrid rGO/Ag q-mesh coatings are shown in Fig. 4a and b, respectively. One can see in Fig. 4b a conformal coating of the q-mesh paths with rGO film. The spectral optical transparency of the system at the main technological stages in the range 400–800 nm is shown in Fig. 4c. The Ag q-mesh electrode with the metallization thickness of 140 nm has the transparency of 90.1%, with the sheet resistance being 12.3 Ω/sq. When spraying the GO film with the thickness 0.01 ml/cm^2 on the Ag q-mesh coating the transparency decreases down to 87.3% with the same sheet resistance. In the process of the GO film reduction the transparency of the hybrid coating decreases down to 82.2%. The coating parameters with various thicknesses of the silver and rGO films are given in Table A1. The ITO film on PET has the transparency of 84% at the wavelength 550 nm, with the sheet resistance being 15 Ω/sq [25]. The hybrid coating has a uniform transmittance spectrum in the range under consideration and the integral transparency of the hybrid coating – rGO/Ag q-mesh – is higher than that of the ITO film on PET. As a result, the hybrid rGO/Ag q-mesh coating has a better optical quality than the ITO film on PET.

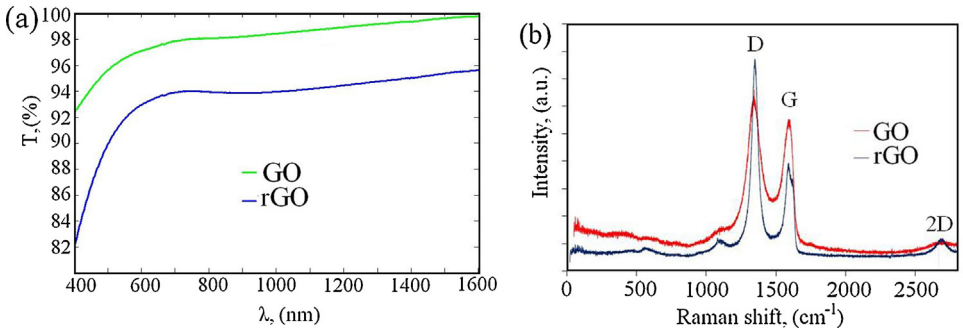

Fig. 3. Spectral dependences of the optical transmittance for GO and rGO films (a). The Raman spectra of GO and rGO films (b).

In the framework of the model of the interaction of two conductive films (providing that the film thickness is smaller than the wavelength of the incident radiation) with electromagnetic radiation of visible range the transmittance coefficient is related with the film sheet resistance by the following expression [26]

$$= \left(1 + \frac{Z_0}{2R_s}\frac{\sigma_{opt}}{\sigma_{dc}}\right)^{-2} = \left(1 + \frac{Z_0}{2R_s F}\right)^{-2} \quad (1)$$

where $Z_0 = 377\,\Omega$, is the vacuum impedance. The coefficient F is used to estimate the quality of the transparent conductive coating. The approximation of the experimental points obtained for the Ag mesh on PET for different thicknesses of the silver films (70–210 nm) shows the parameter F to be about 350 (Fig. 4d). The rGO protective film decreases the value of the parameter F down to 200 due to the reduction of the coating transparency. By comparison, the coefficient F of ITO on glass is equal to ~350, while for ITO film on PET it amounts to ~115 [25]. Other most perspective transparent electrodes has the parameter F smaller than that of silver meshes; for example, for carbon nanotubes the maximum coefficient value was obtained in [27], amounting to 50. For doped CVD graphene the parameter F is equal to 70 [18], and for coatings based on Ag nanowires it amounts to 300 [28].

The chemical and mechanical stability of the Ag q-mesh in aggressive conditions is one of the most important characteristics for a wide range of important applications [10–12,15]. It should be noted that, as contrasted to the coatings based on Ag NW and Cu NW [29,30], the Ag q-mesh coating is stable in atmosphere at room temperature due to the fact that by its properties the Ag q-mesh coating is close to bulk materials (Fig. A4). The protective rGO film allows retaining the integrity and functionality in a chemically aggressive environment. Exposing the Ag q-mesh coating to the aqueous solution of Na_2S (4 wt%) completely etches the coating in 1 min (the inset in Fig. 5a shows the morphology of the etched Ag q-mesh coating), while the hybrid rGO/Ag q-mesh coating after a 30 min exposure increases its sheet resistance from 8.1 to 28.4 Ω/sq, and after a 60 min exposure it increases up to 54.6 Ω/sq (Fig. 5a). The protective rGO film exhibits a significant increase in stability to the aggressive environment as compared to the unprotected coating.

One of the important characteristics of the mesh coatings is its adhesion to the substrate. Fig. 5b presents the results of the tape

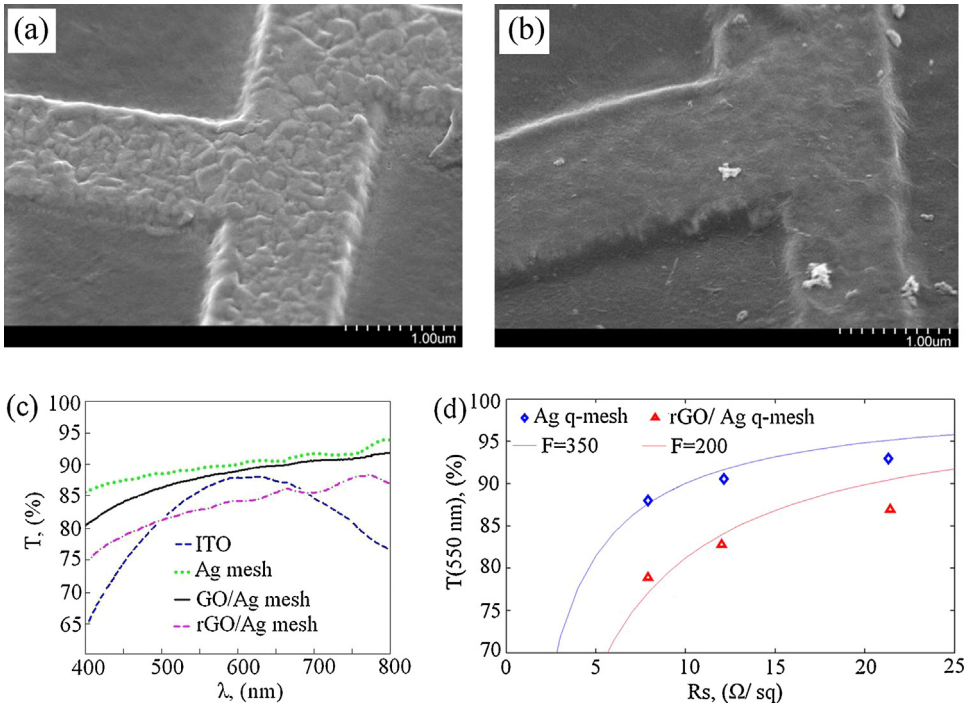

Fig. 4. Morphology of the Ag paths before and after the formation procedure of the protective rGO film (a and b). Spectral dependences of the optical transmittance of the hybrid rGO/Ag q-mesh coating at the main technological stages (c). Approximation of the experimental points of the Ag q-mesh and hybrids rGO/Ag q-mesh coatings, using Eq. (1) (d).

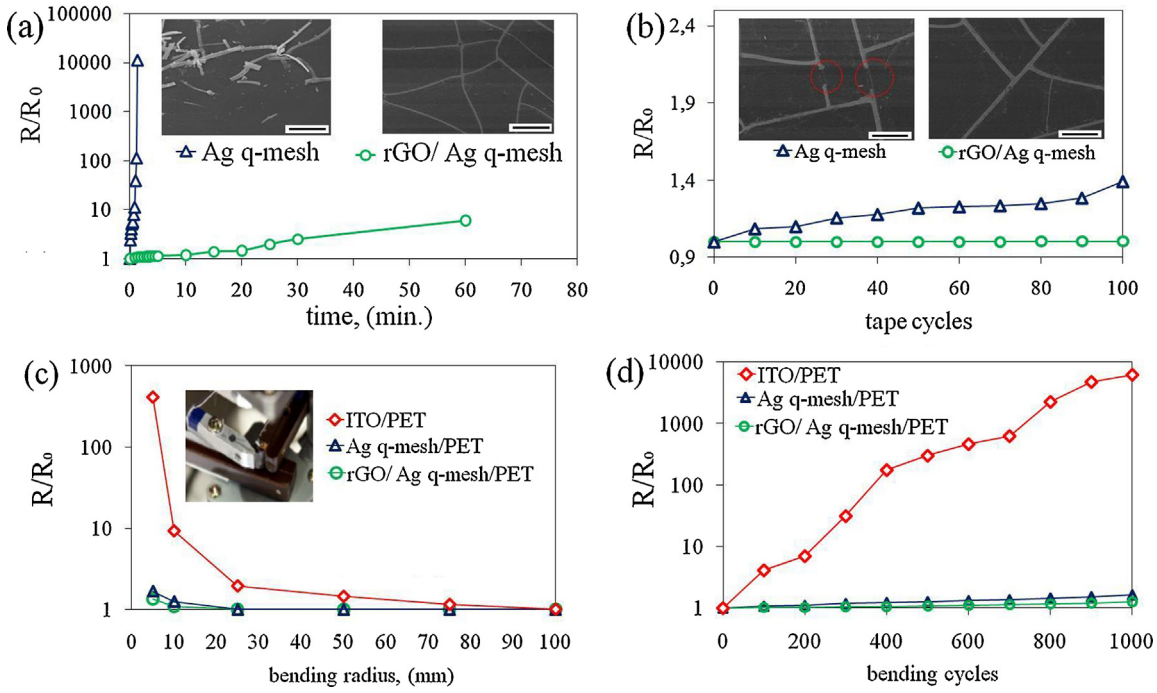

Fig. 5. The durability of hybrid rGO/Ag q-mesh coating. Changing the sheet resistance Ag q-mesh and rGO/Ag q-mesh coatings upon exposure to an aqueous solution of Na_2S (4 wt%). Scale bar: 20 μm (a). Changing the sheet resistance of Ag q-mesh and hybrid rGO/Ag q-mesh coatings as a function of the number of cycles of repeated peeling by scotch tape. Scale bar: 20 μm (b). The effect of bending deformations on the sheet resistance of Ag q-mesh, hybrid rGO/Ag q-mesh coatings and commercial ITO film on PET (c). The effect of cyclic bending deformations with the radius 20 mm on the sheet resistance Ag q-mesh, hybrid rGO/Ag q-mesh coatings and commercial ITO film on PET (d).

test for the Ag q-mesh and rGO/Ag q-mesh coatings. The Ag q-mesh has a strong adhesion to the substrate and after 100 peeling cycles increases its resistance only by 39% due to the partial disruption of the paths. In the case of coatings based on nanowires, the adhesion to the substrate is significantly lower, e.g. after 3 peeling cycles the AgNW film increases its resistance by 3500% [30]. The hybrid rGO/Ag q-mesh coating remains absolutely stable during 100 peeling cycles due to the fact that the rGO sheets have strong adhesion to the surface and additionally pressed the Ag q-mesh.

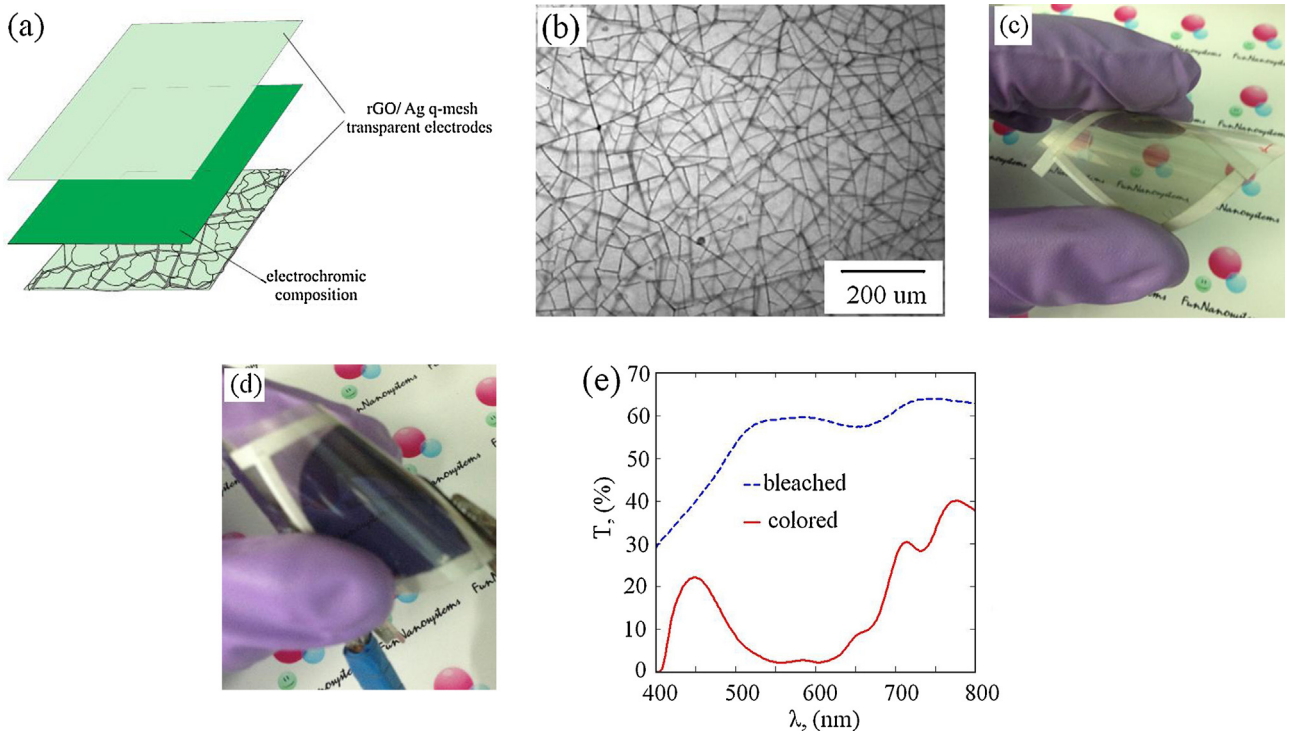

Fig. 6. The scheme and transparent optical microcopy of the electrochromic device (a and b). Images bleached and colored states of the electrochromic device (c and d). Transmittance spectra of the bleached and colored states of the electrochromic devices (e).

An important advantage of hybrid coatings is its increased stability to mechanical deformations (Fig. 5c). Upon bending with the bend radius varying from 100 to 25 mm, the Ag q-mesh and hybrid rGO/Ag q-mesh coatings remain stable and the resistance of ITO film on PET is two times increased. Upon bending with the radius of 5 mm, ITO film on PET loses its conductivity completely, while the resistance of the Ag q-mesh coating increases by 67%, the hybrid rGO/Ag q-mesh coating does so only by 34%.

To study the stability of coatings under operation conditions they were subjected to 1000 runs, with the bend radius being 20 mm (Fig. 5d). The hybrid coating is much more stable to cyclic mechanical impacts, increasing its resistance by 37.7%, while the unprotected Ag q-mesh coating loses 62.5% of its initial conductivity, and ITO film on PET loses its conductivity completely during the investigation process. The rGO flakes play a role of shunting elements and in the case of the mesh disruption during the process of bending deformation they do not allow the damaged section to lose its conductivity completely.

The scheme of the electrochromic device is presented in Fig. 6a. The micrograph of the electrochromic device under transmitted light (Fig. 6b) shows non-periodic superposition of the meshes. As a result, the system does not have a moiré pattern, which improves the optical quality of the electrochromic device. This is one of the advantages of the employed system based on the autoclustered template. When applying the voltage of +1.5 V the cell discolors to saturated blue during 25 s. The polarity of the primary impulse does not matter since the electrochromic reaction proceeds in the whole volume of the sandwich rather than on one of the electrodes as is the case for layered electrochromic cells [31]. With the polarity changing, the cell discolors to white during 30 s. Long time of response is due to the thickness of the electrochromic composition layer (100 μm). Fig. 6c and d present the bleached and colored states of the electrochromic cell. Of importance is the fact that during the process of the cell coloring there is no gradient color structure associated with the electrode mesh character due to the rGO film providing a uniform current contact with the electrochromic composition. Fig. 6e shows the spectral dependences of optical transmittance of the electrochromic cell in the bleached and colored states. The maximum difference of the optical transmittance is observed at the wavelength of 550 nm and is equal to $\Delta T = 56\%$. The electrochromic device based on the hybrid rGO/Ag q-mesh electrodes shows stable operation during a long period of time both in the regime of constant operation and in the cyclic regime while the electrochromic device based on the Ag mesh electrodes starts degradating as early as during the first switching cycle (Fig. A5).

4. Conclusions

A low-cost easily-scaled method of synthesizing hybrid transparent conductive coatings based on the rGO/Ag q-mesh with increased chemical and mechanical stability has been suggested and implemented. The coatings combine low sheet resistance (12.3 Ω/sq), relatively high optical transparency (82.2%). The hybrid rGO/Ag q-mesh coating show high chemical and mechanical stability. The hybrid coatings were tested as electrodes for flexible electrochromic devices. The tested electrochromic device has the difference in transparency between the colored and bleached states of about 56% at the wavelength of 550 nm. The electrochromic device does not lose its functionality upon cyclic mechanical deformations. It is also worth noting that the sandwich system based on hybrid electrodes is deprived of one of the drawbacks of the systems based on electrodes formed using the conventional methods of lithography—moiré pattern.

Appendix A. Supplementary data

Supplementary data associated with this article can be found, in the online version, at http://dx.doi.org/10.1016/j.apsusc.2015.12.182.

References

[1] C.F. Guo, Z. Ren, Flexible transparent conductors based on metal nanowire networks, Mater. Today 18 (2015) 143–154.
[2] S.H. Ahn, L.J. Guo, High-speed roll-to-roll nanoimprint lithography on flexible plastic substrates, Adv. Mater. 20 (2008) 2044–2049.
[3] K.-H. Lee, S.-M. Kim, H. Jeong, Y. Pak, H. Song, J. Park, K.-H. Lim, J.-H. Kim, Y.S. Kim, H.C. Ko, I.K. Kwon, G.-Y. Jung, All-solution-processed transparent thin film transistor and its application to liquid crystals driving, Adv. Mater. 25 (2013) 3209–3214.
[4] J. Zhu, X. Zhu, R. Hoekstra, L. Li, F. Xiu, M. Xue, B. Zeng, K.L. Wang, Metallic nanomesh electrodes with controllable optical properties for organic solar cells, Appl. Phys. Lett. 100 (2012) 143109.
[5] H. Wu, D. Kong, Z. Ruan, P.-C. Hsu, S. Wang, Z. Yu, T.J. Carney, L. Hu, S. Fan, Y. Cui, A transparent electrode based on a metal nanotrough network, Nat. Nanotechnol. 8 (2013) 421–425.
[6] B. Han, K. Pei, Y. Huang, X. Zhang, Q. Rong, Q. Lin, Y. Guo, T. Sun, C. Guo, D. Carnahan, M. Giersig, Y. Wang, J. Gao, Z. Ren, K. Kempa, Uniform self-forming metallic network as a high-performance transparent conductive electrode, Adv. Mater. 26 (2014) 873–877.
[7] R. Gupta, K.D.M. Rao, K. Srivastava, A. Kumar, S. Kiruthika, G.U. Kulkarni, Spray coating of crack templates for the fabrication of transparent conductors and heaters on flat and curved surfaces, ACS Appl. Mater. Interfaces 6 (2014) 13688–13696.
[8] K.T. Park, H.-J. Kim, M.-J. Park, J.-H. Jeong, J. Lee, D.-G. Choi, J.-H. Lee, J.-H. Choi, 13.2% efficiency Si nanowire/PEDOT:PSS hybrid solar cell using a transfer-imprinted Au mesh electrode, Sci. Rep. 5 (2015) 12093.
[9] J. Lee, P. Lee, H. Lee, D. Lee, S.S. Lee, S.H. Ko, Very long Ag nanowire synthesis and its application in a highly transparent, conductive and flexible metal electrode touch panel, Nanoscale 4 (2012) 6408–6414.
[10] P.-C. Hsu, S. Wang, H. Wu, V.K. Narasimhan, D. Kong, H.R. Lee, Y. Cui, Performance enhancement of metal nanowire transparent conducting electrodes by mesoscale metal wires, Nat. Commun. 4 (2013) 2522.
[11] T. Qiu, B. Luo, M. Liang, J. Ning, B. Wang, X. Li, L. Zhi, Hydrogen reduced graphene oxide/metal grid hybrid film: towards high performance transparent conductive electrode for flexible electrochromic devices, Carbon 81 (2015) 232–238.
[12] H.J. Lee, J.H. Hwang, K.B. Choi, S.-G. Jung, K.N. Kim, Y.S. Shim, C.H. Park, Y.W. Park, B.-K. Ju, Effective indium-doped zinc oxide buffer layer on silver nanowires for electrically highly stable, flexible, transparent, and conductive composite electrodes, ACS Appl. Mater. Interfaces 5 (2013) 10397–10403.
[13] Y. Won, A. Kim, D. Lee, W. Yang, K. Woo, S. Jeong, J. Moon, Annealing-free fabrication of highly oxidation-resistive copper nanowire composite conductors for photovoltaics, NPG Asia Mater. 6 (2014) 1–9.
[14] H. Eom, J. Lee, A. Pichitpajongkit, M. Amjadi, J.-H. Jeong, E. Lee, J.-Y. Lee, I. Park, Ag@Ni core–shell nanowire network for robust transparent electrodes against oxidation and sulfurization, Small 10 (2014) 4171–4180.
[15] Z. Chen, S. Ye, A.R. Wilson, Y.-C. Haac, B.J. Wiley, Optically transparent hydrogen evolution catalysts made from networks of copper–platinum core–shell nanowires, Energy Environ. Sci. 7 (2014) 1461–1467.
[16] M.S. Lee, K. Lee, S.-Y. Kim, H. Lee, J. Park, K.-H. Choi, H.-K. Kim, D.-G. Kim, D.-Y. Lee, S.W. Nam, J.-U. Park, High-performance, transparent, and stretchable electrodes using graphene–metal nanowire hybrid structures, Nano Lett. 13 (2013) 2814–2821.
[17] Y. Zhu, Z. Sun, Z. Yan, Z. Jin, J.M. Tour, Rational design of hybrid graphene films for high-performance transparent electrodes, ACS Nano 5 (2011) 6472–6479.
[18] S. Bae, H. Kim, Y. Lee, X. Xu, J.-S. Park, Y. Zheng, J. Balakrishnan, T. Lei, H.R. Kim, Y.I. Song, Y.-J. Kim, K.S. Kim, B. Özyilmaz, J.-H. Ahn, B.H. Hong, S. Iijima, Roll-to-roll production of 30-inch graphene films for transparent electrodes, Nat. Nanotechnol. 5 (2010) 574–578.
[19] I.N. Kholmanov, S.H. Domingues, H. Chou, X. Wang, C. Tan, J.-Y. Kim, H. Li, R. Piner, A.J.G. Zarbin, R.S. Ruoff, Reduced graphene oxide/copper nanowire hybrid films as high-performance transparent electrodes, ACS Nano 7 (2013) 1811–1816.
[20] S. Jeong, L. Hu, H.R. Lee, E. Garnett, J.W. Choi, Y. Cui, Fast and scalable printing of large area monolayer nanoparticles for nanotexturing applications, Nano Lett. 10 (2010) 2989–2994.
[21] L. Pauchard, Patterns caused by buckle-driven delamination in desiccated colloidal gels, Europhys. Lett. 74 (2006) 188–194.
[22] W.S. Hummers, R.E. Offeman, Preparation of graphitic oxide, J. Am. Chem. Soc. 80 (1958) 1339.
[23] H.-J. Shin, K.K. Kim, A. Benayad, S.-M. Yoon, H.K. Park, I.-S. Jung, M.H. Jin, H.-K. Jeong, J.M. Kim, J.-Y. Choi, Y.H. Lee, Efficient reduction of graphite oxide by sodium borohydride and its effect on electrical conductance, Adv. Funct. Mater. 19 (2009) 1987–1992.

[24] G. Eda, M. Chhowalla, Chemically derived graphene oxide: towards large-area thin-film electronics and optoelectronics, Adv. Mater. 22 (2010) 2392–2415.
[25] http://www.prochema.cn/.
[26] D.S. Hecht, L.B. Hu, G. Irvin, Emerging transparent electrodes based on thin films of carbon nanotubes, graphene, and metallic nanostructures, Adv. Mater. 23 (2011) 1482–1513.
[27] D.S. Hecht, A.M. Heintz, R. Lee, L. Hu, B. Moore, C. Cucksey, S. Risser, High conductivity transparent carbon nanotube films deposited from superacid, Nanotechnology 22 (2011) 075201.
[28] T.Y. Kim, Y.W. Kim, H.S. Lee, H. Kim, W.S. Yang, K.S. Suh, Uniformly interconnected silver-nanowire networks for transparent film heaters, Adv. Funct. Mater. 23 (2013) 1250–1255.
[29] A.R. Rathmell, M. Nguyen, M. Chi, B.J. Wiley, Synthesis of oxidation-resistant cupronickel nanowires for transparent conducting nanowire networks, Nano Lett. 12 (2012) 3193–3199.
[30] B. Deng, P.-C. Hsu, G. Chen, B.N. Chandrashekar, L. Liao, Z. Ayitimuda, J. Wu, Y. Guo, L. Lin, Y. Zhou, M. Aisijiang, Q. Xie, Y. Cui, Z. Liu, H. Peng, Roll-to-roll encapsulation of metal nanowires between grapheme and plastic substrate for high-performance flexible transparent electrodes, Nano Lett. 15 (2015) 4206–4213.
[31] C.-C. Liao, F.-R. Chen, J.-J. Kai, Electrochromic properties of nanocomposite WO_3 films, Solar Energy Mater. Solar Cells 91 (2007) 1282–1288.